Supporting Information for
Hydrogen Donation but not Abstraction by a Tyrosine (Y68) During Endoperoxide Installation by Verruculogen Synthase (FtmOx1)

Noah P. Dunham,[1,4] José M. Del Río Pantoja,[1,5] Bo Zhang,[2,6] Lauren J. Rajakovich,[1,5] Benjamin D. Allen,[1,3] Carsten Krebs,[1,2] Amie K. Boal,[1,2] and J. Martin Bollinger, Jr.[1,2]

[1]Department of Biochemistry and Molecular Biology, [2]Department of Chemistry, and [3]The Huck Institutes for Life Sciences, The Pennsylvania State University, University Park, PA 16802, United States

[4]Present Address: Division of Chemistry and Chemical Engineering, California Institute of Technology, Pasadena, CA 91125

[5]Present Address: Department of Chemistry and Chemical Biology, Harvard University, Cambridge, MA 02138

[6]Present Address: Renewable Energy Group, Inc., 600 Gateway Blvd, South San Francisco, CA 94080

Materials and Methods

General methods

Liquid chromatography detected by mass spectrometry (LC-MS) was carried out on a 1260 series LC system in tandem with a 1260 series triple quadrupole mass spectrometer (Agilent Technologies). Gas chromatography detected by mass spectrometry (GC-MS) was carried out on a GCMS-QP5000 system (Shimadzu). All DNA sequencing was performed at The Pennsylvania State University Nucleic Acid Core Facility. The fumitremorgin B substrate was purchased from Quality Phytochemicals LLC (East Brunswick, NJ) and the verruculogen product standard was purchased from Enzo Life Sciences (Farmingdale, NY). $Fe(NH_4)_2(SO_4)_2 \cdot 6H_2O$ was purchased from J. T. Baker (Philipsburg, NJ). All reagents were used directly as obtained. The molecular weight and purity of wild-type (wt) FtmOx1 and single-site (Y $\rightarrow$ F) variants were assessed by SDS-polyacrylamide gel electrophoresis (SDS-PAGE) with visualization by Coomassie blue staining.

Construction of FtmOx1 expression vectors

The DNA sequence encoding FtmOx1 from *Aspergillus fumigatus* was codon-optimized for expression in *Escherichia coli*, synthesized, and ligated with the pET28a vector at its *Nde*I and *BamH*I restriction sites (GenScript). The synthetic gene encodes an N-terminal metal-ion affinity tag, consisting of 21 amino acids (M G S S H H H H H H S S G L V P R G S H M) with an internal His_6 metal-binding sequence. The full gene sequence is:

ATGGGCAGCAGCCATCATCATCATCATCACAGCAGCGGCCTGGTGCCGCGCGGCAGCCATATGATG
ACCGTGGATAGCAAACCGCAACTGCAACGTCTGGCGGCGGATGCGGATGTGGACCGTATGTGCCG
TCTGCTGGAGGAAGATGGTGCGTTCATCCTGAAGGGCCTGCTGCCGTTCGACGTGGTTGAGAGCTT
TAACCGTGAACTGGATGTGCAGATGGCGATCCCGCCGCCGAAAGGCGAGCGTCTGCTGGCGGACA
AGTACCCGCCGCACTTCAAATATGTGCCGAACGTTGCGACCACCTGCCCGACCTTTCGTAACACCGT
GCTGATCAACCCGGTTATCCACGCGATTTGCGAAGCGTACTTCCAACGTACCGGCGATTATTGGCTG
AGCGCGGCGTTTCTGCGTGAGATTGAAAGCGGTATGCCGGCGCAGCCGTTTCACCGTGACGATGC
GACCCACCCGCTGATGCACTATCAGCCGCTGGAGGCTCCGCCGGTTAGCCTGAGCGTTATCTTCCC
GCTGACCGAGTTTACCGAGGAAAACGGCGCGACCGAAGTTATTCTGGGTAGCCATCGTTGGACCGA
GGTGGGTACCCCGGAACGTGATCAAGCGGTTCTGGCGACCATGGACCCGGGTGATGTGCTGATCG
TTCGTCAACGTGTGGTTCATGCGGGTGGCGGTAACCGTACCACCGCGGGCAAGCCGCGTCGTGTG
GTTCTGGCGTACTTCAACAGCGTGCAGCTGACCCCGTTTGAAACCTATCGTACCATGCCGCGTGAGA
TGGTGGAAAGCATGACCGTTCTGGGCCAACGTATGCTGGGTTGGCGTACCATGAAACCGAGCGATC
CGAACATCGTTGGTATTAACCTGATTGATGACAAGCGTCTGGAAAATGTTCTGCAACTGAAAGCGGC
GGACAGCCCGGCG

A second FtmOx1 expression construct containing an N-terminal SUMO fusion and an intervening TEV cleavage site was created by standard recombinant DNA methods. *Bsa*I sites were added on the 5' and 3' ends of the FtmOx1 gene via PCR using primers shown below (*Bsa*I recognition site underlined):

Forward: 5'-ACAAGGTCTCATGACCGTGGATAGCAAACCG-3'

Reverse: 5'-ACAAGGTCTCTCACGCCGGGCTGTCCG-3'

The amplified gene was inserted into a home-built pBA0028 vector, a modified pET28a plasmid with a SUMO tag and TEV cleavage site encoded between the N-terminal metal-ion-affinity tag and protein encoded by the inserted gene. Matching *Bsa*I sites were incorporated into linearized vector using primers shown below (*Bsa*I recognition site underlined):

Forward: 5'-ACAAGGTCTCGCGTGAGATCCGGCTGCTAACAAAG-3'

Reverse: 5'-ACAAGGTCTCGGTCATGGATTGGAAGTACAGGTTTTCC-3'

The full gene sequence of the FtmOx1 SUMO-TEV construct is:

ATGCATCATCACCATCACCACGGTTCTTCTATGGCTAGCATGTCGGACTCAGAAGTCAATCAAGAAG
CTAAGCCAGAGGTCAAGCCAGAAGTCAAGCCTGAGACTCACATCAATTTAAAGGTGTCCGATGGATC
TTCAGAGATCTTCTTCAAGATCAAAAAGACCACTCCTTTAAGAAGGCTGATGGAAGCGTTCGCTAAAA
GACAGGGTAAGGAAATGGACTCCTTAAGATTCTTGTACGACGGTATTAGAATTCAAGCTGATCAGAC
CCCTGAAGATTTGGACATGGAGGATAACGATATTATTGAGGCTCACAGAGAACAGATTGGTGGGATC
GAGGAAAACCTGTACTTCCAATCCATGACCGTGGATAGCAAACCGCAACTGCAACGTCTGGCGGCG
GATGCGGATGTGGACCGTATGTGCCGTCTGCTGGAGGAAGATGGTGCGTTCATCCTGAAGGGCCTG
CTGCCGTTCGACGTGGTTGAGAGCTTTAACCGTGAACTGGATGTGCAGATGGCGATCCCGCCGCCG
AAAGGCGAGCGTCTGCTGGCGGACAAGTACCCGCCGCACTTCAAATATGTGCCGAACGTTGCGACC
ACCTGCCCGACCTTTCGTAACACCGTGCTGATCAACCCGGTTATCCACGCGATTTGCGAAGCGTACT
TCCAACGTACCGGCGATTATTGGCTGAGCGCGGCGTTTCTGCGTGAGATTGAAAGCGGTATGCCGG
CGCAGCCGTTTCACCGTGACGATGCGACCCACCCGCTGATGCACTATCAGCCGCTGGAGGCTCCG
CCGGTTAGCCTGAGCGTTATCTTCCCGCTGACCGAGTTTACCGAGGAAAACGGCGCGACCGAAGTT
ATTCTGGGTAGCCATCGTTGGACCGAGGTGGGTACCCCGGAACGTGATCAAGCGGTTCTGGCGACC
ATGGACCCGGGTGATGTGCTGATCGTTCGTCAACGTGTGGTTCATGCGGGTGGCGGTAACCGTACC
ACCGCGGGCAAGCCGCGTCGTGTGGTTCTGGCGTACTTCAACAGCGTGCAGCTGACCCCGTTTGAA
ACCTATCGTACCATGCCGCGTGAGATGGTGGAAAGCATGACCGTTCTGGGCCAACGTATGCTGGGT
TGGCGTACCATGAAACCGAGCGATCCGAACATCGTTGGTATTAACCTGATTGATGACAAGCGTCTGG
AAAATGTTCTGCAACTGAAAGCGGCGGACAGCCCGGCGTGA

The protein sequences of the FtmOx1 TEV construct before and after cleavage are shown below.

Before TEV cleavage (TEV cleavage site is highlighted in red):

MHHHHHHGSSMASMSDSEVNQEAKPEVKPEVKPETHINLKVSDGSSEIFFKIKKTTPLRRLMEAFAKRQ
GKEMDSLRFLYDGIRIQADQTPEDLDMEDNDIIEAHREQIGGIEENLYFQSMTVDSKPQLQRLAADADVDR
MCRLLEEDGAFILKGLLPFDVVESFNRELDVQMAIPPPKGERLLADKYPPHFKYVPNVATTCPTFRNTVLI
NPVIHAICEAYFQRTGDYWLSAAFLREIESGMPAQPFHRDDATHPLMHYQPLEAPPVSLSVIFPLTEFTEE
NGATEVILGSHRWTEVGTPERDQAVLATMDPGDVLIVRQRVVHAGGGNRTTAGKPRRVVLAYFNSVQLT
PFETYRTMPREMVESMTVLGQRMLGWRTMKPSDPNIVGINLIDDKRLENVLQLKAADSPA

After TEV cleavage:

SMTVDSKPQLQRLAADADVDRMCRLLEEDGAFILKGLLPFDVVESFNRELDVQMAIPPPKGERLLADKYP
PHFKYVPNVATTCPTFRNTVLINPVIHAICEAYFQRTGDYWLSAAFLREIESGMPAQPFHRDDATHPLMHY
QPLEAPPVSLSVIFPLTEFTEENGATEVILGSHRWTEVGTPERDQAVLATMDPGDVLIVRQRVVHAGGGN
RTTAGKPRRVVLAYFNSVQLTPFETYRTMPREMVESMTVLGQRMLGWRTMKPSDPNIVGINLIDDKRLE
NVLQLKAADSPA

The Y68F, Y74F, Y140F, and Y224F substitutions were introduced individually by inverse PCR site-directed mutagenesis[1] using the FtmOx1 pET28a plasmid as template. The relevant primer sequences for each variant are listed below. The sequences of the resulting plasmids were verified.

Y68F_forward: 5'-TTTCCGCCGCACTTCAAATATGTG-3'

Y68F_reverse: 5'-CTTGTCCGCCAGCAGACGCTC-3'

Y74F_forward: 5'-TTTGTGCCGAACGTTGCGAC-3'

Y74F_reverse: 5'-TTTGAAGTGCGGCGGGTAC-3'

Y140F_forward: 5'-TTTCAGCCGCTGGAGGCTC-3'

Y140F_reverse: 5'-GTGCATCAGCGGGTGG-3'

Y224F_forward: 5'-TTTTTCAACAGCGTGCAGCTGAC-3'

Y224F_reverse: 5'-ACACGACGCGGCTTGCC-3'

Growth, Expression, and Purification of FtmOx1

E. coli BL21 (DE3) competent cells were transformed with the pET28a-based expression vectors for wt or variant FtmOx1 by the heat-shock method, and the resulting transformants were selected on LB plates supplemented with kanamycin (50 μg/mL). A single colony was used to inoculate 150 mL of LB medium supplemented with 50 μg/ml kanamycin. This culture was grown overnight at 37 °C. A 25-mL inoculum from the starter culture was transferred to 1 L of LB medium supplemented with 50 μg/mL kanamycin. Cultures were initially grown at 37 °C. Once they had reached an optical density of ~ 0.6, the temperature of the incubator was set to 18 °C. Expression was induced by addition of IPTG to a final concentration of 1 mM. The cultures were allowed to grow for an additional 16-18 h at 18 °C. Cells were harvested by centrifugation at 8,000*g* for 15 min and flash frozen in liquid N_2. The cell pellets were stored at -80 °C until they were used.

All purification steps were performed at 4 °C. In a typical preparation, 30 g of cell paste was re-suspended in ~ 200 mL 100 mM Tris-HCl, pH 7.5. Lysozyme and phenylmethylsulfonyl fluoride were added to final concentrations of 0.1 mg/mL and 1 mM, respectively. The suspension was stirred on ice to homogeneity, and the cells were lysed by sonication in intervals of 10 s on and 30 s off for a total sonication time of ~ 8 min. The cell debris was separated by centrifugation at 22,000*g* for 30 min. The supernatant was loaded onto ~ 18 mL of Ni-NTA resin and washed with ~ 150 mL of 100 mM Tris-HCl, pH 7.5. The protein was eluted from the resin with 250 mM imidazole, 100 mM Tris-HCl, pH 7.5, and concentrated using a 10 kDa molecular weight cut-off centrifugal concentrators (Pall Corporation, Port Washington, NY) before a single round of dialysis against 5 mM EDTA, 100 mM Tris-HCl, pH 7.5. This step was implemented to remove any metal ions retained through expression and purification. Two subsequent rounds of dialysis were performed against 100 mM Tris-HCl, pH 7.5. The protein was further concentrated (as above), and its final concentration was determined by its absorbance at 280 nm using a calculated molar absorption coefficient of 26,930 M^{-1} cm^{-1} (https://web.expasy.org/protparam/).

Growth, Expression, Purification, and Characterization of 3,3-d_2*-L-Tyr FtmOx1*

E. coli WU-36 competent cells harboring the pAR1219 vector (encoding the T7 RNA polymerase and ampicillin resistance marker) were transformed with the pET28a-based FtmOx1 expression vector, and colonies were allowed to grow on LB plates supplemented with kanamycin (50 µg/mL) and ampicillin (100 µg/mL). A single colony was used to inoculate 150 mL of M9 minimal medium supplemented with 40 µg/mL 3,3-d_2-L-Tyr, 50 µg/ml kanamycin, and 50 µg/ml ampicillin. This culture was incubated overnight at 37 °C. A 25-mL aliquot of this starter culture was used to inoculate 1 L of M9 medium supplemented with 40 µg/ml 3,3-d_2-L-Tyr, 50 µg/ml kanamycin, and 50 µg/ml ampicillin. Cultures were grown at 37 °C to an optical density of 0.6–0.8. The cultures were placed in an ice-water bath for ~ 30 min prior to induction of expression by addition of IPTG to a final concentration of 170 µM. Cultures were allowed to grow for an additional 16-18 h at 18 °C. Cells were harvested by centrifugation at 8,000*g* for 20 min and flash frozen in liquid N_2. The protein was purified as described above.

The incorporation of 3,3-d_2-L-Tyr into FtmOx1 was confirmed by mass spectrometric analysis at the Penn State University Proteomics and Mass Spectrometry Core Facility. Samples containing 10 µg of

protein were digested with trypsin in the presence of *tris*-(2-carboxyethyl)phosphine and iodoacetamide. A 2-µL aliquot of the digest was loaded onto an Acclaim PepMap100 trapping column (100 µm × 2 cm, C18, 5 µm, 100 Å, Thermo Fisher Scientific) at a flow rate of 5 µL/min using 2% aqueous acetonitrile, 0.1% formic acid as mobile phase. The peptides were separated on an Acclaim PepMap RSLC column (75 µm × 15 cm, C18, 2 µm, 100 Å, Thermo Fisher Scientific) with a 30-min 2% - 35% linear gradient of acetonitrile in water containing 0.1% formic acid. The gradient was delivered by a Dionex Ultimate 3000 nano-LC system (Thermo Fisher Scientific) at 300 nL/min.

An LTQ Orbitrap Velos mass spectrometer (Thermo) was set to acquire the data on the top 15 precursors using the 'Nth order double play' method. The following method parameters were used: full FT MS scan over the 350-1700 *m/z* range at R 60,000, followed by 10 ion-trap MS^2 scans with CID activation. Only the precursors with charge states +2 and higher were selected for MS^2; monoisotopic precursor selection was enabled (repeat 1, repeat duration 30 s, exclusion duration 90 s), and the isolation window was set at 3 *m/z*. Polysiloxane ion at 445.1200 *m/z* was used as a lock mass. The AGC target values were $1.0e^4$ for MS^n in the ion trap and $1.0e^6$ for FTMS with maximum inject times of 50 ms and 1000 ms, respectively. One microscan was used in both the ion trap and the Orbitrap.

The mass spectra were processed using Proteome Discoverer version 1.3.0.339 (Thermo Fisher Scientific). The incorporation of deuteriated tyrosine was confirmed by specifying a dynamic modification "Label:$^2H_2$, +2.012 Da (Y)"; other modifications were carbamidomethylation of Cys (static) and oxidation of Met (dynamic). The protein database contained 4535 sequences: *E. coli* (expression system), common contaminants, and FtmOx1. Precursor tolerance was 10 ppm; fragment tolerance was 0.8 Da (ion trap); two missed cleavages were allowed; and minimum peptide confidence was set to "high" in the result filters.

For the accompanying MALDI-TOF analysis, mass spectra were acquired on a Bruker Ultraflextreme MALDI TOF-TOF instrument using a factory-configured instrument method for the reflector positive-ion detection over the 700 – 3500 *m/z* range. Laser power attenuation was optimized to achieve the best signal. The instrument was calibrated with a bovine serum albumin tryptic digest mixture (Protea), and a 10 mg/mL solution of α-cyano-4-hydroxycinnamic acid in 50% acetonitrile containing 1% trifluoroacetic acid was used as the matrix for both the calibration mixture and the sample.

LC-MS analysis of FtmOx1 reaction products

Reaction components were separated on an Agilent Zorbax Extend-C18 column (4.6 x 50 mm, 1.8 µm particle size) initially in 70% solvent A (0.1% formic acid in water) and 30% solvent B (acetonitrile). The column was developed at a flow rate of 0.8 mL/min. A gradient of 70% to 0% solvent A was applied from 0 min (the time of injection) to 12 min. The column was then returned to 70% solvent A by a linear gradient from 12 min to 13 min and washed with 70% solvent A from 13 min to 16 min before the next injection. Detection of fumitremorgin B and the fumitremorgin B-derived products was achieved by electrospray ionization in the positive-ion mode (ESI+).

GC-MS detection of prenol

Assay mixtures were separated on an Agilent DB-23 column (60 m x 25 mm x 25 µm) at a column inlet pressure of 100 kPa and column flow rate of 0.7 mL/min. The injection and interface temperatures were set to 175 °C and 220 °C, respectively. The oven temperature was initially set to 80 °C for 3 min. From 3 min to 14.5 min, the temperature was increased by a linear gradient from 80 °C to 225 °C. The interface temperature to the mass spectrometer was set to 220 °C. Detection of prenol was achieved by electron ionization (EI).

Table S1. Relevant statistics from the PDB validation report from the previously-solved structure of FtmOx1 in complex with fumitremorgin B (PDB: 4ZON). The Z-score can be calculated for each bond length and angle in a component of a structural model (in this case, of the substrate) to reveal metrics that differ by more than 2 standard deviations from their mean values ($|Z| > 2$), potentially reflecting anomalies. The root-mean-square value of the Z-scores (RMSZ) for the whole molecule is expected to lie between 0 and 1; RMSZs > 1 can imply over-fitting of the experimental data.[2] The real space correlation coefficient (RSCC) and real space R value (RSR) are two metrics that assess how well the calculated electron density map from the modeled ligand (fumitremorgin B) and the observed electron density map from the experimental diffraction data agree. RSCC values less than 0.8 indicate a poor fit of the model to the original data. RSR values of 0 indicate perfect agreement of the model to the map. Values approaching or exceeding 0.4 indicate poor agreement of the model and map.[3]

Fumitremorgin B geometry		
	Bond lengths	Bond angles
$\#\|Z\| > 2$	5 (16%)	8 (23%)
RMSZ	2.00	1.71
Fit of fumitremorgin B to crystallographic data		
Real space correlation coefficient (RSCC)	0.66	
Real space R value (RSR)	0.52	

Table S2. Summary of data collection and refinement statistics for the reported x-ray crystal structures of FtmOx1-Y140F.

	His-tagged FtmOx1-Y140F·Fe(II)·2OG	**FtmOx1-Y140F·Fe(II)**
Data collection		
Wavelength	0.97857 Å	0.97857 Å
Space group	$P2_12_12_1$	$P2_12_12_1$
Cell dimensions		
a, b, c (Å)	73.512, 79.362, 91.511	73.884, 78.068, 91.444
α, β, γ (°)	90.00, 90.00, 90.00	90.00, 90.00, 90.00
Resolution (Å)	50.00-1.92 (1.95-1.92)	50.00-1.55 (1.58-1.55)
R_{merge}	0.080 (0.850)	0.040 (0.417)
$< I/\sigma >$	21.7 (2.1)	29.9 (3.2)
$CC_{1/2}$	0.833	0.850
Completeness (%)	98.8 (93.7)	96.5 (97.5)
Redundancy	6.7 (5.7)	4.3 (3.7)
Refinement		
Resolution (Å)	50.00-1.92	50.00-1.55
No. reflections	35350	74662
R_{work} / R_{free}	0.2084/0.2516	0.1809/0.2175
No. atoms		
Protein	4483	4481
Ion/Ligand	22	2
Water	41	306
B-Factors		
Protein	23.1	16.9
Ion/Ligand	26.8	16.6
Water	14.3	22.9
r.m.s. deviations		
Bond lengths (Å)	0.008	0.007
Bond angles (°)	1.175	1.126
Ramachandran statistics (%)		
favored	96.6	98.0
outliers	0.2	0
PDB accession code	6OXH	6OXJ

Scheme S1. Two reactions of the COX isoforms. (**A**) Peroxidase reaction converting prostaglandin G_2 (PGG_2) to prostaglandin H_2 (PGH_2) and activating for the endoperoxide synthase reaction by formation of a Tyr• (**B**) Catalytic endoperoxidation reaction converting arachidonic acid (AA) to prostaglandin G_2 (PGG_2).

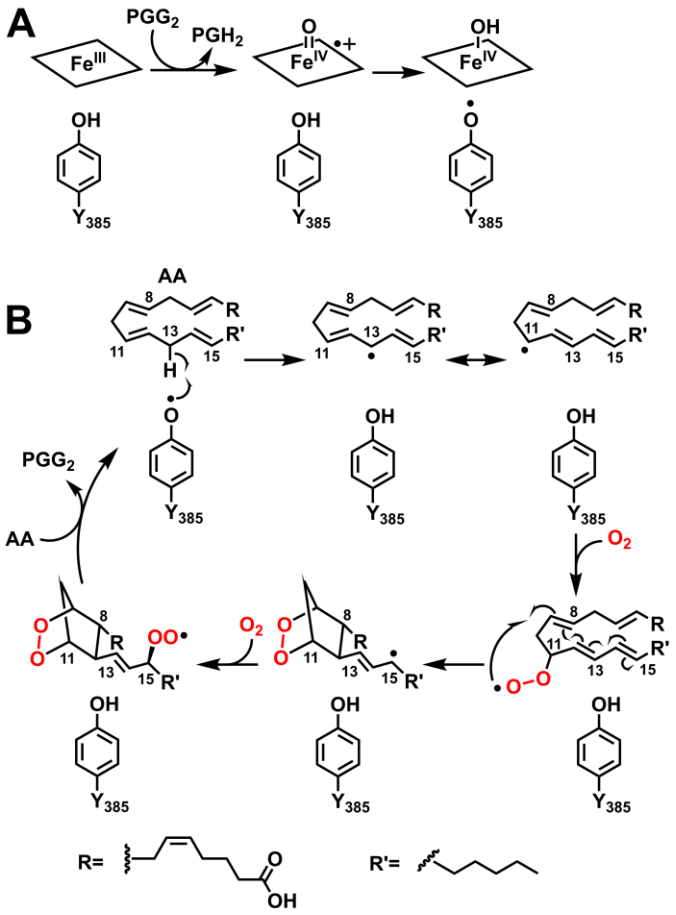

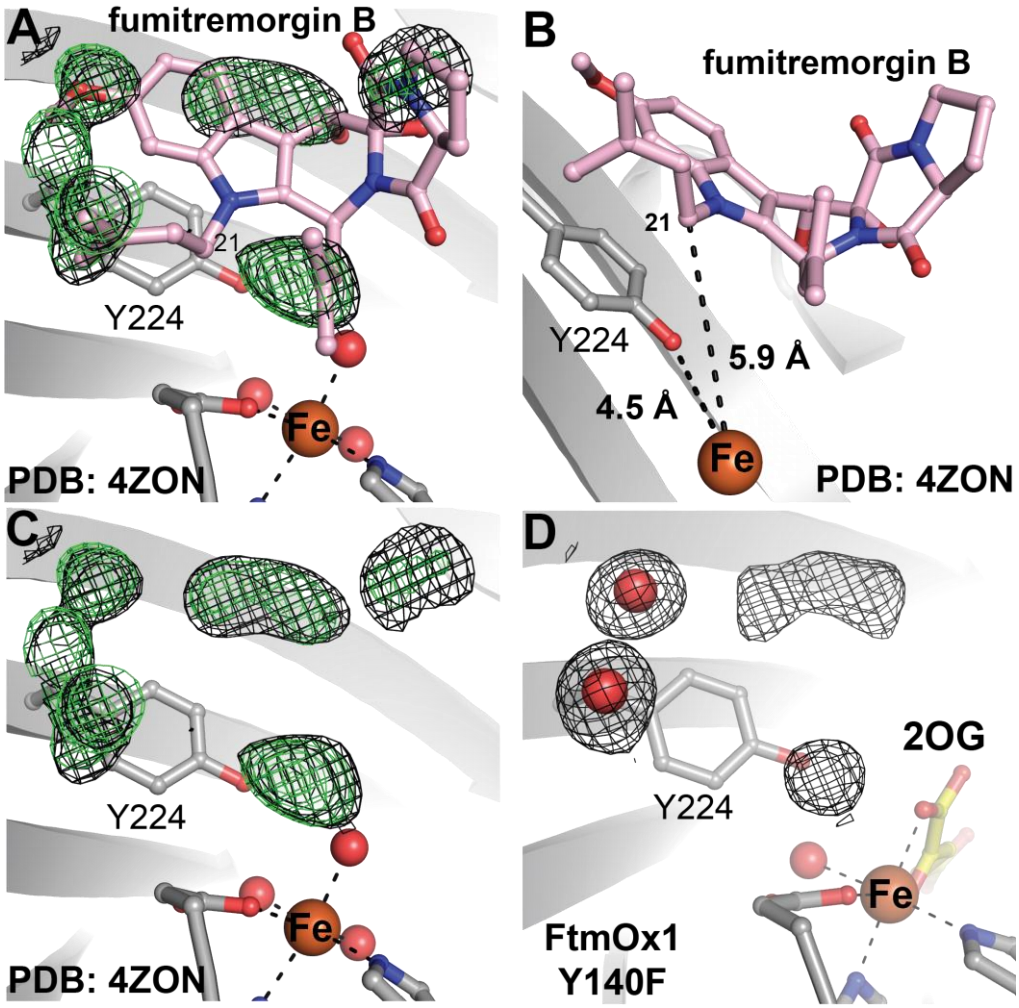

Figure S1. Comparative analysis of the published x-ray crystal structure of FtmOx1 (PDB accession code 4ZON) and the structure of its Y140F variant obtained in this work. (**A**) View of the active site as modeled in 4ZON, with fumitremorgin B bound. The coordinates and structure factors were downloaded directly from the RCSB PDB and used as-is or as input for additional refinement in Refmac5 after deletion of the 35 atoms in chain A associated with the substrate. A $2F_o$-F_c map (black mesh) generated from the deposited structure factors is shown contoured to 1.0 σ. An F_o-F_c omit map (green mesh), calculated by deletion of fumitremorgin B and subsequent refinement in Refmac5 against deposited structure factors, is shown contoured to 3.0 σ. Neither map supports the modeling of fumitremorgin B in the active site. (**B**) Disposition of the iron cofactor, Y224, and HAT donor C21 suggested by the previous paper, giving Fe–O-Y224 and Fe–C21 distances of 4.5 Å and 5.9 Å, respectively. (**C**) Comparison of the F_o-F_c map from the 4ZON structure (green mesh, 3.0 σ) to the $2F_o$-F_c map generated from our x-ray diffraction experiments with FtmOx1 Y140F (black mesh, 1.0 σ). (**D**) Demonstration that much of the extra active-site density seen in both datasets can reasonably be modeled as ordered water molecules.

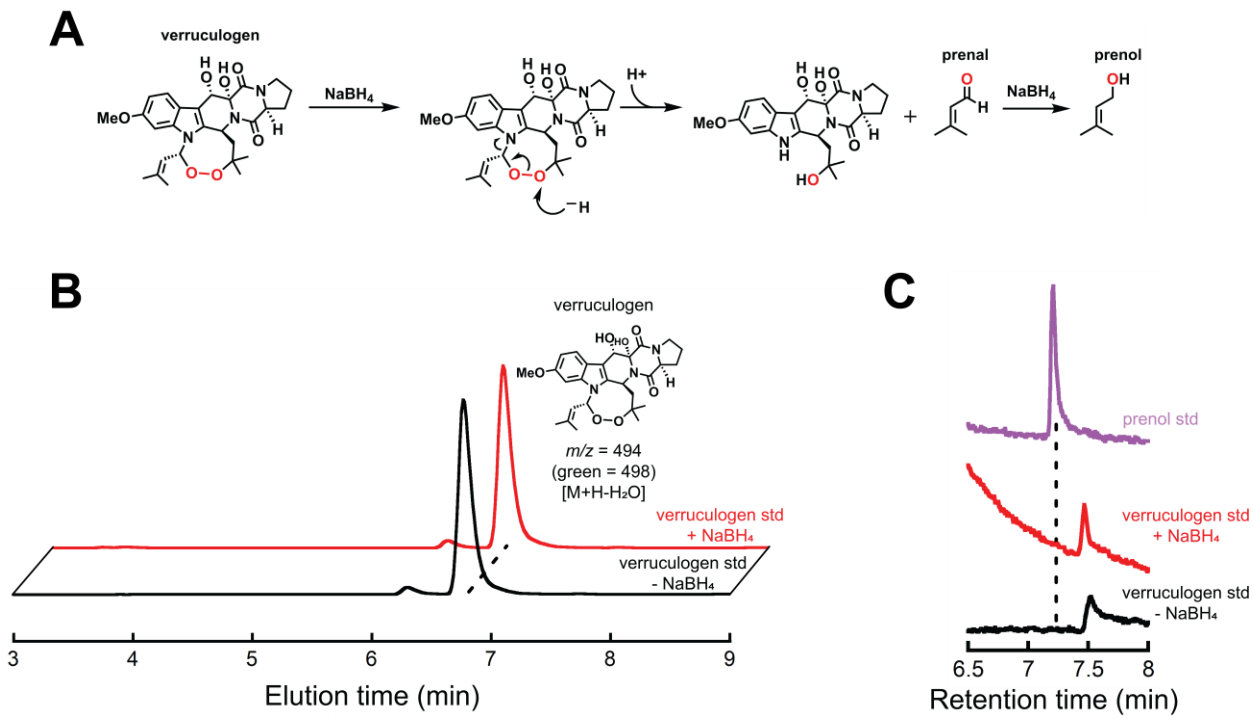

Figure S2. Control experiment to verify that the observed incorporation of ^{18}O from $^{18}O_2$ into prenal by FtmOx1 proceeds by enzymatic C21 hydroxylation (rebound) and not by $NaBH_4$-mediated cleavage of the endoperoxide product. (**A**) Possible mechanism of breakdown of the verruculogen product by $NaBH_4$ to prenol with incorporation of ^{18}O from $^{18}O_2$. (**B**) LC-MS analysis of a control sample prepared by treatment of the verruculogen standard with $NaBH_4$ (*red trace*) and comparison to the standard before treatment with $NaBH_4$ (*black trace*). The near identity of the red and black traces shows that the endoperoxide product is unreactive toward even a large excess of $NaBH_4$ under the conditions of the workup. (**C**) GC-MS analysis confirming that $NaBH_4$ does not cause decomposition of the verruculogen endoperoxide with release of prenol. We can therefore conclude that the ^{18}O-prenol detected in **Figure 2C** results from hydroxylation of C21 of the fumitremorgin B substrate.

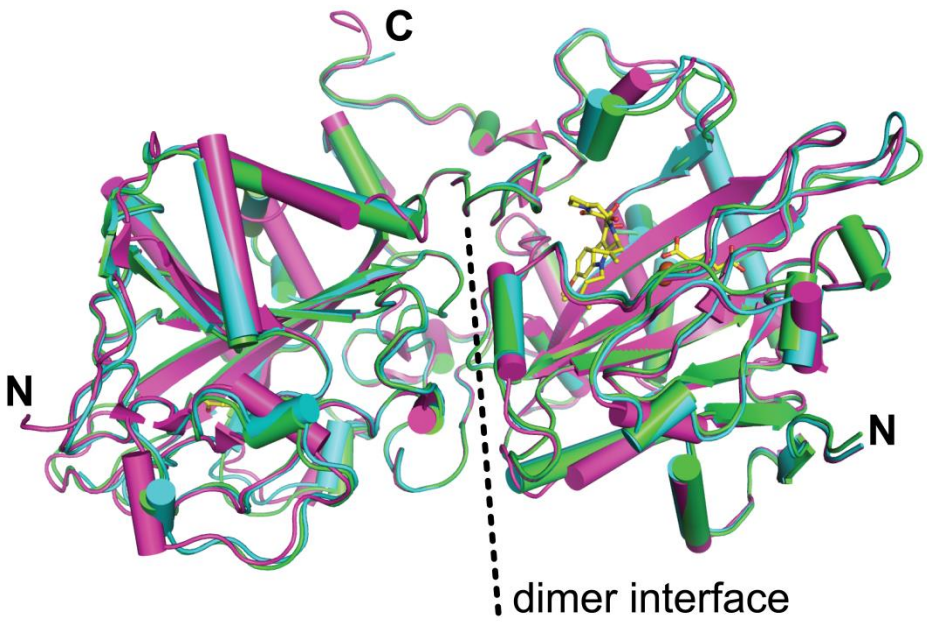

Figure S3. A cartoon diagram showing the secondary-structure-matching superposition of the 4ZON structure (purple) with our structures of FtmOx1-Y140F, with (green, rmsd = 0.61 for 283 Cα atoms) and without (teal, rmsd = 0.39 for 285 Cα atoms) the N-terminal affinity tag. Each structure contains two molecules in the asymmetric unit (ASU). The rmsd values are reported for one of the two monomers in the ASU.

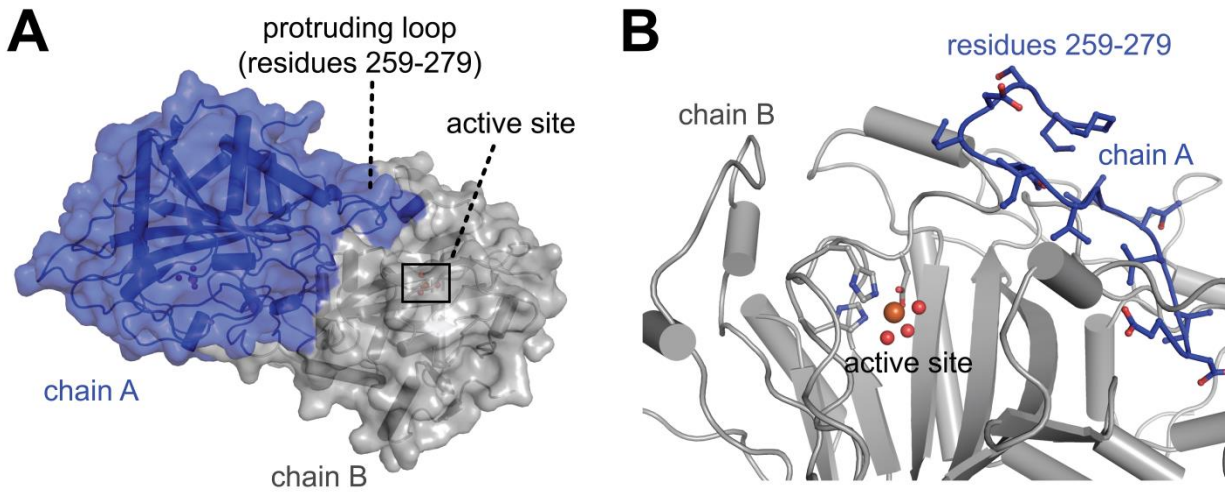

Figure S4. Quaternary interfaces, seen in the FtmOx1 x-ray crystal structures, that could affect substrate binding. (**A**) In each subunit, a loop region (residues 259-279) protrudes near the active site of the neighboring subunit. We considered the possibility that this conformation might prevent binding of the substrate, particularly in soaking experiments, in the crystal lattice. However, the arrangement is symmetric and appears to be part of a true dimer interface that persists despite variation in space group and crystal packing. (**B**) A zoomed-in view of the protruding loop, with selected side chains displayed in the ball-and-stick format.

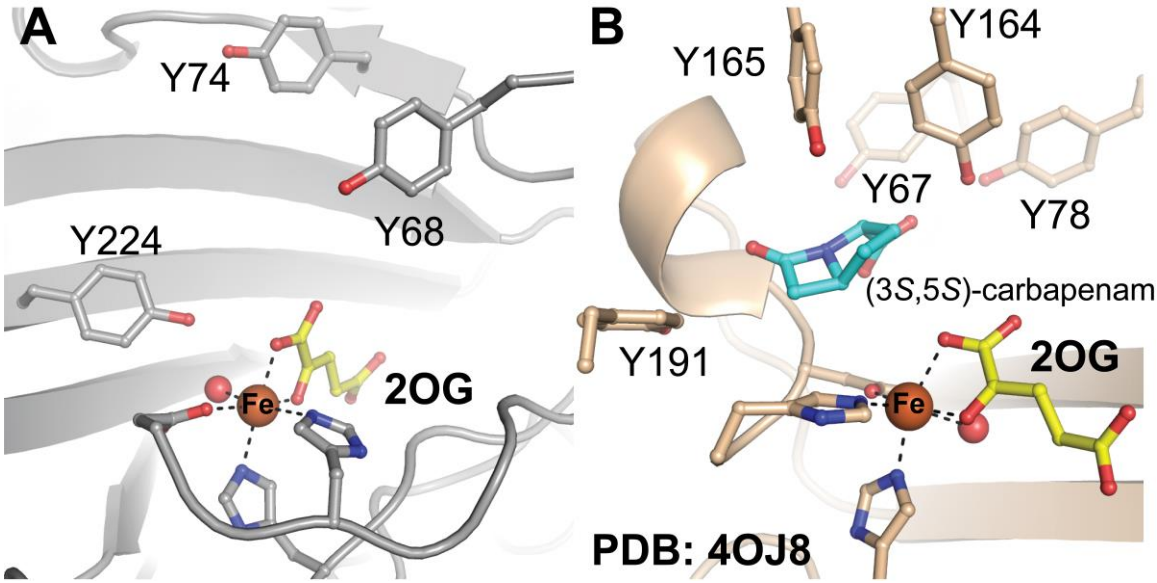

Figure S5. Comparison of tyrosine residues in the active site of FtmOx1-Y140F (**A**) and CarC (**B**).

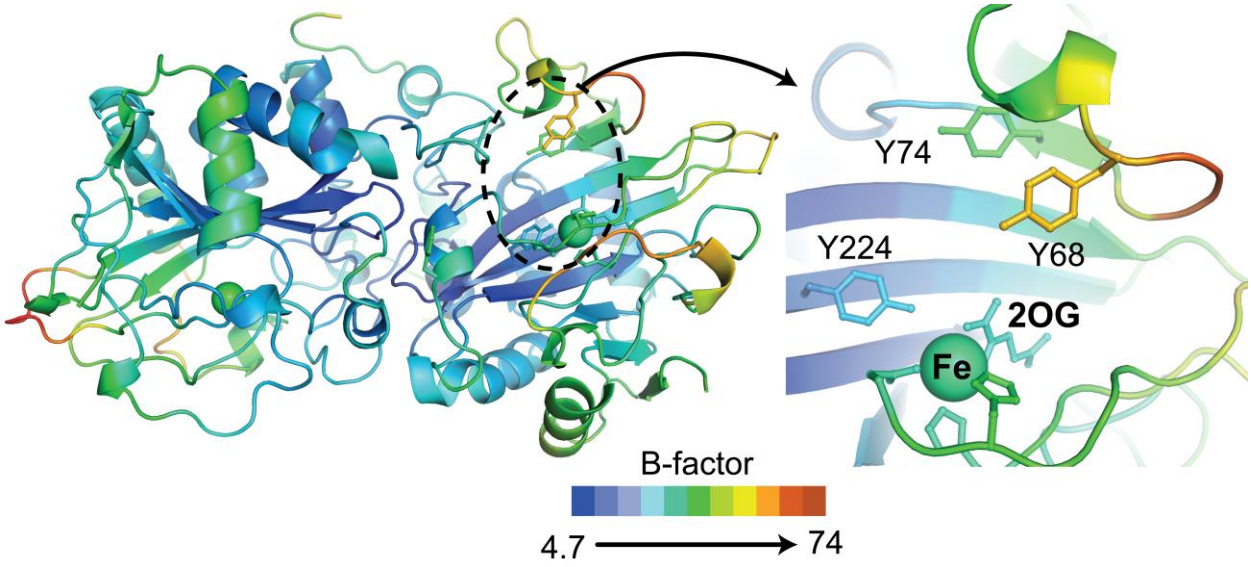

Figure S6. Views of the FtmOx1-Y140F structure, colored according to B-factor. (*Left*) Full view of the entire dimer. (*Right*) Zoomed-in view of the loop containing Y68 and Y74. The elevated *B*-factors of this loop in comparison to the rest of the protein suggest that the region may be flexible.

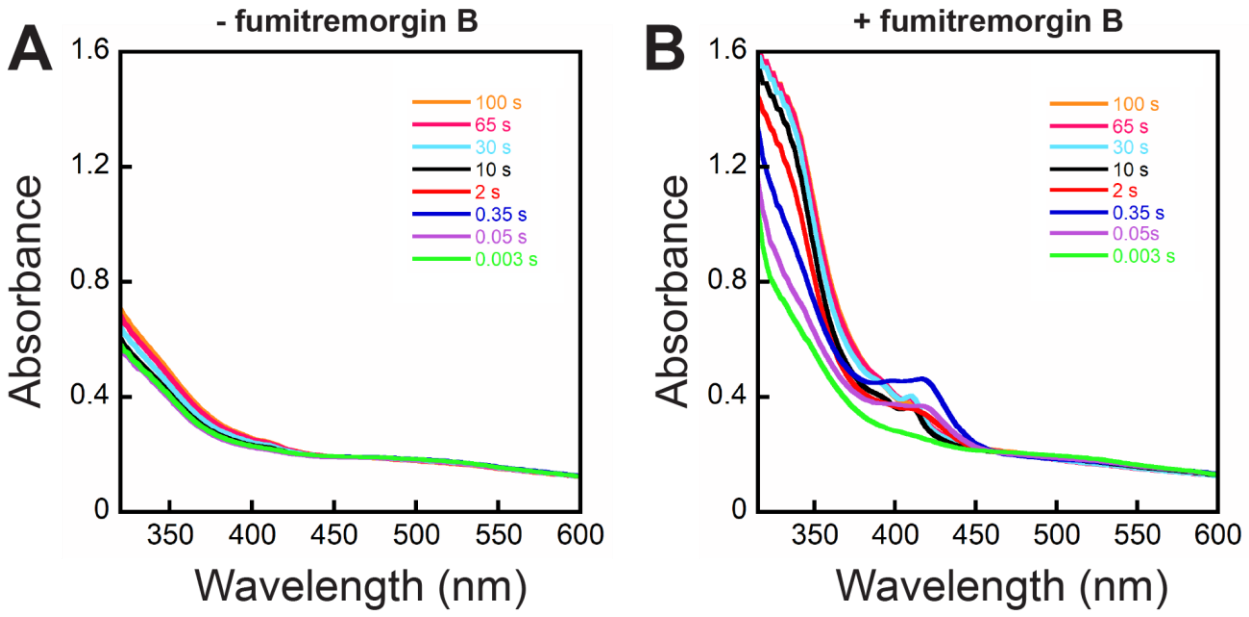

Figure S7. Stopped-flow absorption experiments demonstrating "substrate triggering" in the FtmOx1-Y140F reaction. (**A**) Absorption spectra obtained at the indicated reaction times after mixing at 5 °C of a solution containing 1.2 mM FtmOx1, 1.2 mM $Fe(NH_4)_2(SO_4)_2$, and 10 mM 2OG with an equal volume of O_2-saturated buffer. (**B**) Spectra after mixing of the same solutions but with 0.4 mM fumitremorgin B also included in the enzyme solution.

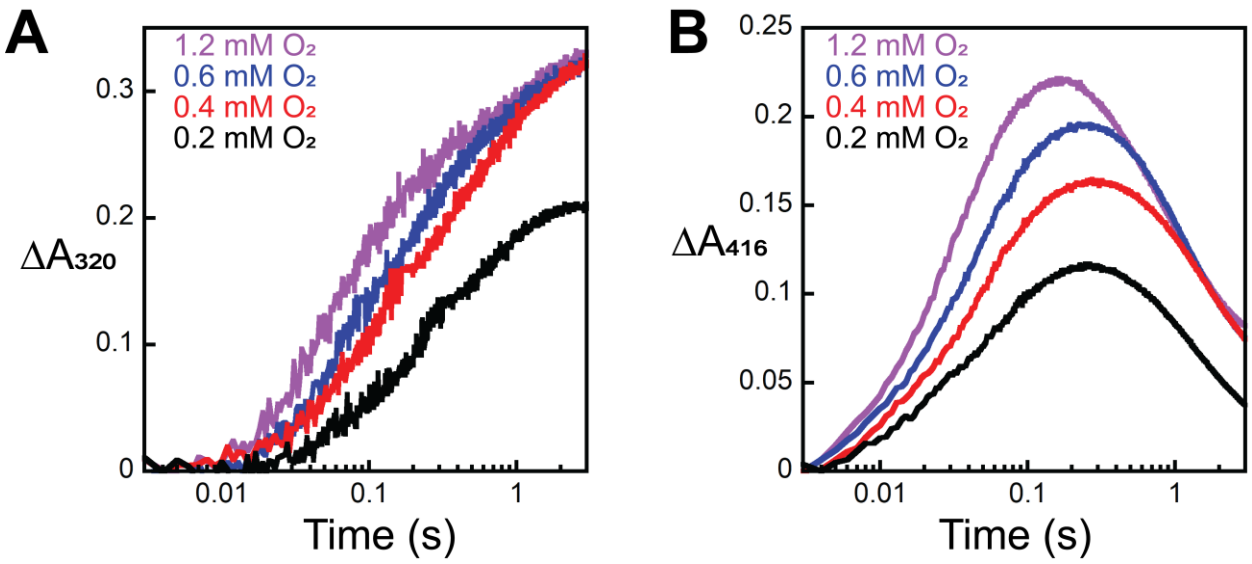

Figure S8. Stopped-flow absorption analysis of the FtmOx1 reaction for possible accumulation of precursors to the Fe(III)/Tyr• state. (**A**) Absorbance-versus-time races at 320 nm (often used to monitor the ferryl complexes of Fe/2OG oxygenases) following initiation of the reaction with varying concentrations of O_2. (**B**) Absorbance-versus-time races at 416 nm, the wavelength of maximum absorbance of the first Tyr•, from the same reactions. Chlorite dismutase (Cld) was used to generate O_2 *in situ* as previously described.[4] The reactions were initiated by mixing at 5 °C of an anoxic solution of 1.2 mM FtmOx1, 1.2 mM $Fe(NH_4)_2(SO_4)_2$, 0.4 mM fumitremorgin B, 10 mM 2OG, and 0.02 mM chlorite dismutase with an equal of anoxic buffer containing 0.4 mM, 0.8 mM, 1.2 mM, or 2.4 mM $NaClO_2$.

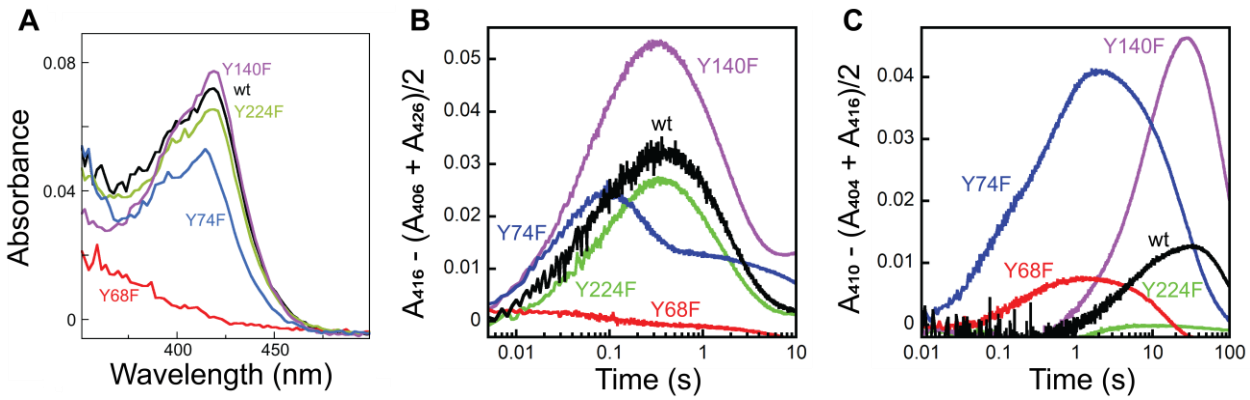

Figure S9. Mathematical analysis of raw stopped-flow data to extract insight into the spectra and kinetics of individual transient species in the reactions of the FtmOx1 wt and Y → F variant proteins. (**A**) Kinetic difference spectra obtained by subtracting the first reliable spectrum (3 ms) from the spectra of later reaction times [0.050 s for wt (*black*), Y68F (*red*), and Y224F (*green*); 0.020 s for Y74F (*blue*) and Y140F (*purple*)]. Minor scalar adjustments (< 0.01) to individual spectra were made for ease of comparison. (**B**, **C**) Plots of peak-heights at 416 nm (**B**) and 410 nm (**C**) as a function of time for the same reactions intended to extract the kinetics of the first and second Tyr•. Note that (1) the reaction of the Y68F variant produces almost no signal in panel **B**, suggesting that this residue is the site of the first radical, and (2) the reaction of the Y224F variant produces almost no signal in panel **C**, suggesting that this residue is the site of the second radical. The Y74F and Y140F substitutions perturb the kinetics of both species without eliminating either.

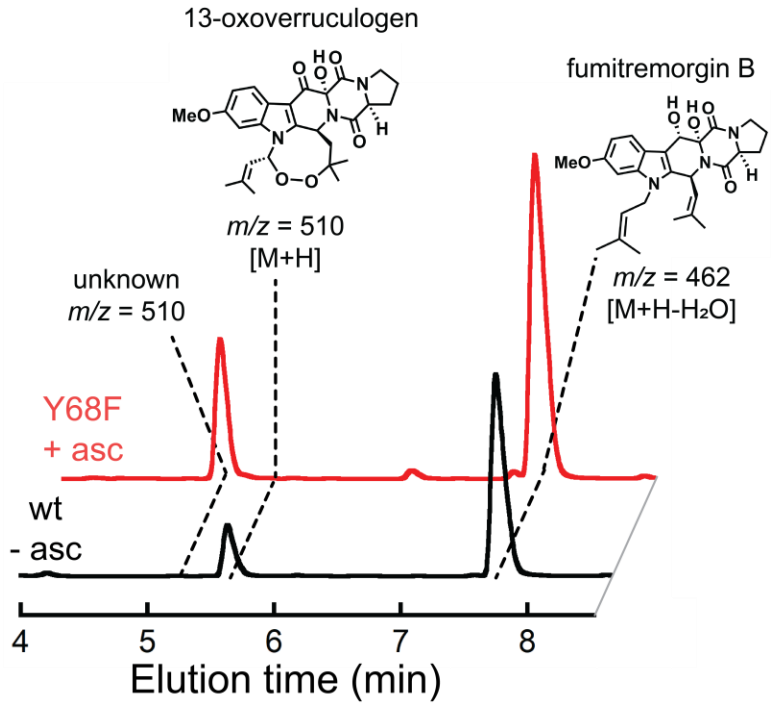

Figure S10. Demonstration by LC-MS analysis that the major product generated by the FtmOx1-Y68F protein (*m*/*z* = 510) is not the 13-oxo-verrculogen ketone product of further two-electron oxidation of the primary verruculogen product. Note that the FtmOx1-Y68F product elutes ahead of the 13-oxo-verruculogen compound produced by the wt enzyme in the absence of ascorbate. The peak for fumitremorgin B is also shown as an elution standard.

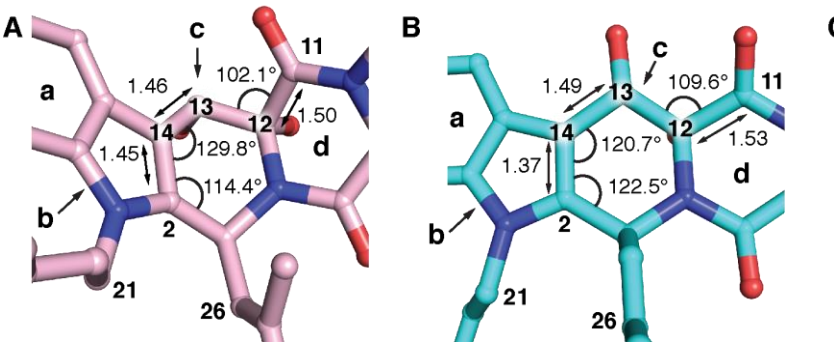

C

bond	JLigand	AceDRG	ideal
C2-C14	1.45 Å	1.37 Å	1.36 Å
C13-C14	1.46 Å	1.49 Å	1.50 Å
C11-C12	1.50 Å	1.53 Å	1.54 Å
C3-C2-C14	114.4°	122.5°	126.3°
C2-C14-C13	129.8°	120.7°	122.9°
C3-C2-C14	102.1°	109.6°	109.7°

Figure S11. (**A**) Selected bond lengths and bond angles near the six-membered **c** ring of fumitremorgin B in the published FtmOx1 crystal structure (PDB: 4ZON). Analysis with the Mogul extension of Mercury (The Cambridge Crystallographic Data Centre) revealed significant bond length/angle outliers in comparison to the Cambridge Structural Database molecular library; the top three are shown in this panel. We speculate that these outliers were present in a JLigand-generated model of the substrate and persisted in the deposited x-ray structure because they could not be corrected by fitting into a high-quality experimental electron density map. The resulting distortion in the **c** ring gives rise to the overall curled conformation of the molecule illustrated in Fig. S12. Notably, the central ring conformation is strikingly different in the experimental x-ray structure of verruculogen. (**B**) A different starting model for fumitremorgin B was generated from the verruculogen x-ray crystal structure after editing in AceDRG to remove the endoperoxide bridge. This structure was used as input for the docking model in **Figure 9**, because it exhibits more idealized values for the selected bond lengths and bond angles flagged in the JLigand model in panel A.

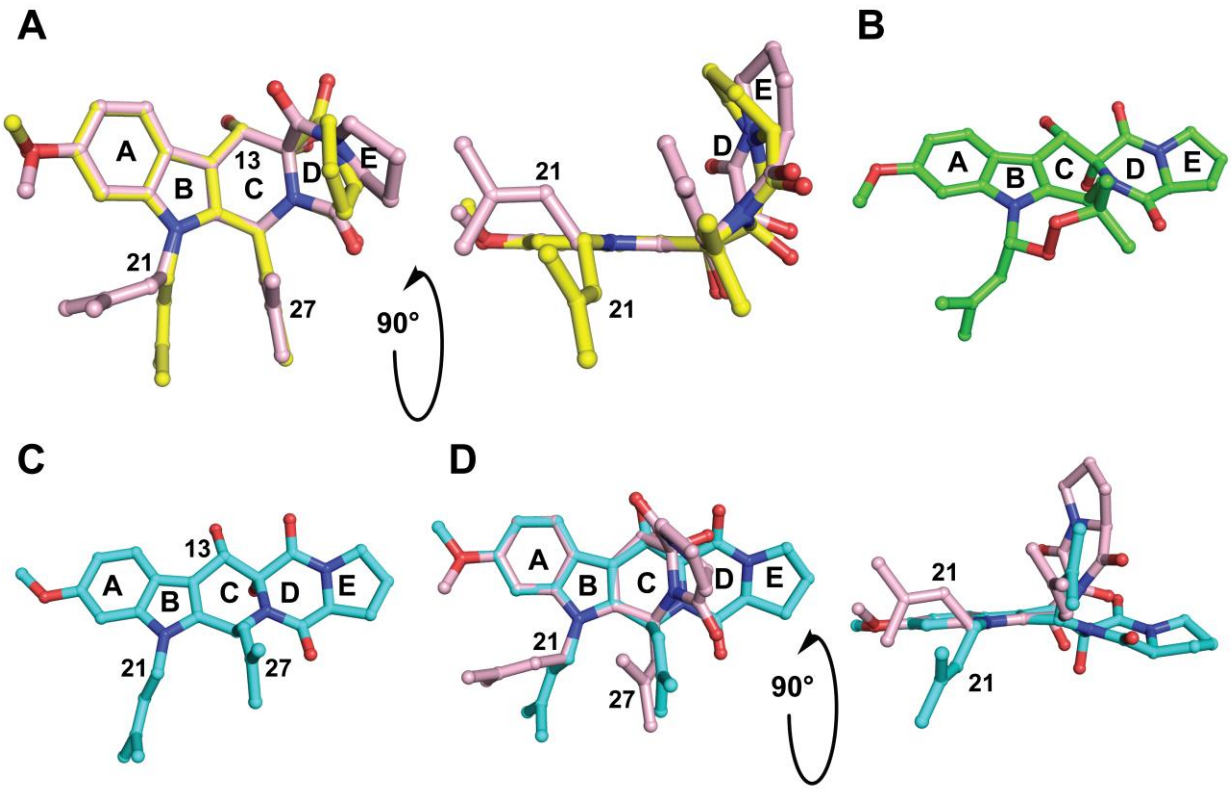

Figure S12. Structural models of the FtmOx1 substrate (fumitremorgin B) and product (verruculogen). (**A**) Overlay of the fumitremorgin B conformation from the active site of the 4ZON structure (*pink*) and a model created using the JLigand extension of the COOT software package (*yellow*).[5,6] The structures align very well (rmsd = 0.03), and both display a distorted conformation about the 2,5-diketopiperazine ring (ring D). This analysis is the basis for our speculation that a similar model served as the starting point in the 4ZON structure and that the absence of high-quality experimental electron density arising from the substrate in the active site left this conformation unchanged in structural refinement. (**B**) Model of verruculogen from its crystal structure. (**C**) The structure in **B** was used as a starting point to generate a model of fumitremorgin B for the purposes of docking into the experimental structure of FtmOx1•Fe(II)•2OG. The endoperoxide moiety was deleted, and the structure was minimized using Avogadro. (**D**) overlay of our fumitremorgin B starting model (*teal*) with fumitremorgin B from the active site of 4ZON (*pink*).

References

(1) Hemsley, A.; Arnheim, N.; Toney, M. D.; Cortopassi, G.; Galas, D. J. A simple method for site-directed mutagenesis using the polymerase chain reaction. *Nucleic Acids Res* **1989**, *17 (16)*, 6545.

(2) Bruno, I. J.; Cole, J. C.; Kessler, M.; Luo, J.; Motherwell, W. D. S.; Purkis, L. H.; Smith, B. R.; Taylor, R.; Cooper, R. I.; Harris, S. E.; Orpen, A. G. Retrieval of crystallographically-derived molecular geometry information. *J. Chem. Inf. Comput. Sci.* **2004**, *44 (6)*, 2133.

(3) Smart, O. S.; Horsky, V.; Gore, S.; Varekova, R. S.; Bendova, V.; Kleywegt, G. J.; Velankar, S. Validation of ligands in macromolecular structures determined by X-ray crystallography. *Acta Crystallogr D* **2018**, *74*, 228.

(4) Dassama, L. M. K.; Yosca, T. H.; Conner, D. A.; Lee, M. H.; Blanc, B.; Streit, B. R.; Green, M. T.; DuBois, J. L.; Krebs, C.; Bollinger, J. M., Jr. O_2-evolving chlorite dismutase as a tool for studying O_2-utilizing enzymes. *Biochemistry* **2012**, *51 (8)*, 1607.

(5) Emsley, P.; Cowtan, K. Coot: model-building tools for molecular graphics. *Acta Crystallogr D* **2004**, *60*, 2126.

(6) Lebedev, A. A.; Young, P.; Isupov, M. N.; Moroz, O. V.; Vagin, A. A.; Murshudov, G. N. JLigand: a graphical tool for the CCP4 template-restraint library. *Acta Crystallogr D* **2012**, *68 (Pt 4)*, 431.